EFDA–JET–CP(10)08/44

M.P. Gryaznevich, Y.Q. Liu, T.C. Hender, D.F. Howell, I.T.Chapman,
C.D. Challis, S.P. Pinches, E. Joffrin, H.R. Koslowski, P. Buratti,
F. Villone, E. Solano and JET-EFDA contributors

Determination of Plasma Stability using Resonant Field Amplification in JET

Determination of Plasma Stability using Resonant Field Amplification in JET

M.P. Gryaznevich[1], Y.Q. Liu[1], T.C. Hender[1], D.F. Howell[1], I.T. Chapman[1], C.D. Challis[1], S.P. Pinches[1], E. Joffrin[2], H.R. Koslowski[3], P. Buratti[4], F. Villone[4], E. Solano[5] and JET-EFDA contributors*

JET-EFDA, Culham Science Centre, OX14 3DB, Abingdon, UK

[1]EURATOM-CCFE Fusion Association, Culham Science Centre, OX14 3DB, Abingdon, OXON, UK
[2]Association Euratom – CEA, Cadarache, Saint-Paul-lez-Durance, France
[3]Assoziationen Euratom-Forschungszentrum Jülich, Germany
[4]EURATOM-ENEA Fusion Association, Italy
[5]Asociación EURATOM-CIEMAT, Madrid, Spain.
** See annex of F. Romanelli et al, "Overview of JET Results", (23rd IAEA Fusion Energy Conference, Daejon, Republic of Korea (2010)).*

Preprint of Paper to be submitted for publication in Proceedings of the 23rd IAEA Fusion Energy Conference, Daejon, Republic of Korea (10th October 2010 - 16th October 2010)

ABSTRACT.

The Resonant Field Amplification has been systematically measured on JET using active MHD spectroscopy to probe plasma stability at high and low beta and compared with theoretical predictions. At high beta, RFA has been used to identify the ideal no-wall beta limit in several advanced regimes: the hybrid regime, with low magnetic shear and q(0) close to 1, and high-beta plasmas being developed for steady-state application, with low or reversed magnetic shear and $1.0 < q_{min} < 2.5$, including regimes with and without internal transport barriers (ITBs). RFA has been measured as a plasma response to applied helical fields with toroidal number *n = 1*, and the diagnostic has been extended to the *n=2* probing. It was found experimentally and explained theoretically that the beta limit strongly depends on the current density and q profiles, and in particular on the q(0) value for monotonic q-profiles or q_{min} for reversed shear profiles, and on details of the current density profile near the plasma edge. At low beta, RFA has been observed prior to onset of a fast rotating *n=1* mode, and during ELM-free periods prior to the first ELM either after L-H transition or after long ELM-free periods during a pulse. These observations confirm that the measured increase in the RFA in some cases (e.g. at low beta) may be not connected with the no-wall beta limit associated with the RWM, but may reflect a proximity to other stability thresholds. A model retaining information about the plasma response in comparison with the kinetic damping model is presented to describe the resonant field amplification in the presence of a stable RWM.

1. RFA MEASUREMENTS ON JET AT HIGH β_N

The Resonant Field Amplification has been systematically measured on JET, mainly in high-β advanced regimes [1]. Two pairs of external Error Field Correction Coils, Fig.1, were powered from two independent power supplies allowing application of a stationary or rotating *n = 1* magnetic field. To measure the RFA, EFCC currents of 200 – 800A (x16 turns) have been used with frequency from 3Hz to as high as 60Hz. Either pair of EFCCs in Octants 1–5 or 3–7 was used to produce an *n = 1* field and a plasma response was measured with a combination of midplane in-vessel saddle loops in Octants 1, 3, 5 and 7. To measure the plasma response at β_N close or below the no-wall limit, a sophisticated technique of the synchronous detection was used. Fourier analysis of the measured saddle loop signals has been performed and the ratio of amplitudes (at the probing frequency) of the n = 1 combination of signals measured by saddle loops situated in an octant orthogonal to the octants of the powered EFCCs to those at the EFCCs position, has been taken as the RFA.

$$RFA = (B_r - B_r^{vac})/B_r^{vac}$$

Details of the diagnostics set-up can be found in [1]. Recently, this diagnostics has been upgraded to allow n = 2 probing.

The Resonant Field Amplification has been most systematically measured on JET in two domains favourable for ITER steady-state operations: broad q-profiles with $q_{min} \sim 1$ and $q_{min} \sim 2$. MARS-

F code modelling reproduces RFA data at low and high beta and suggests a new method of how the RFA data should be used to determine the no-wall limit experimentally [3]. It is important to diagnose the beta limit to prevent/avoid the most dangerous pressure-driven disruptions in JET and ITER. Although there is no strong evidence of a beta-limit on JET connected with the RWM even at β_N~4 and performance was limited by an internal n=1 mode [9], RFA has been found to be a good indicator of the overall stability, predicting the appearance of a limiting mode. The destabilisation of the limiting mode may be connected with a local increase in the pressure gradient (weak transient ITB) at q_{min}~1 or due to evolution of the q-profile (at higher q_{min}).

The observed, Fig.2, and predicted (by the MARS-F modelling) decrease in the RFA threshold with increasing q_{min} is in general in good agreement with a similar dependence of the experimentally achieved highest beta values on JET, although optimisation with the aim of avoiding the limiting mode sometimes produced higher beta values [1]. We have also observed a systematic downward shift of the RFA-measured thresholds compared to the beta limits according to the ideal MHD MARS-F predictions [2]. Very similar limits to those obtained with MARS-F have been predicted in [1] by the MHD code MISHKA-1.

The first attempt to find the reason for this difference was to provide a better understanding of the correlation between the observed increases in the RFA at certain beta, e.g. the RFA threshold, with the ideal no-wall limit. A new method of the experimental no-wall beta limit identification using the logarithmic derivative of the RFA amplitude versus, β_N, $dLn|RFA|/d\beta_N$, [2] has been proposed. The MARS-F simulations show that the logarithmic derivative reaches its peak at a β_N very close to the corresponding no-wall limit. Further modelling results also show that the new logarithmic definition of the RFA threshold is robust against the wall time constant and the wall geometry. The accuracy of the application of this method strongly depends on the quality of the probing signal, and substantial upgrade in the EFCC power supplies has been recently undertaken in order to improve the performance.

Another reason for the discrepancy may be an inaccuracy of the equilibrium reconstruction, since it is well understood that the no-wall beta limit is sensitive to the details of the plasma pressure and q profiles. So detailed modelling of the effect of such details on the no-wall limit has been performed and, for example, confirmed the importance of details of the current density profile on the no-wall beta limit, rather than integral parameters (e.g. internal inductance), which is also observed in experiments, Fig.2 (insert). This means that changes in the current density profile only can affect the beta limit if these changes result in a destabilisation of some (e.g. peeling) modes. Due to peeling modes, the ideal beta limit can significantly reduce. A more carefully tuned reconstruction procedure where a nonvanishing equilibrium current density at the plasma edge causes instability of the *n=1* ideal peeling mode at low plasma pressure resulted in a more reasonable agreements between the experimental data and the modelling results. We should note that this beta limit change does not depend on any damping mechanisms neither on a non-linear coupling of modes during their evolution. However, the RFA amplitude and the absolute value of the $dLn|RFA|/d\beta_N$ will depend

on these factors, as shown, for example, in [3] for the influence of the plasma rotation on RFA.

MARS-F has been also used to model low-n large amplitude RFA peaks observed in JET plasmas below the ideal no-wall limit, Fig.3 (left). Here the *n = 1* RFA increase is seen at β_N below the RFA threshold, which is seen as a steep increase in RFA associated with the ideal no-wall limit. It is unlikely that these peaks contain a dominant contribution from the response of a stable RWM. Besides, experimental evidence suggests a correlation between these low beta RFA signals and the ELM free period prior to the first ELM [1]. The resonant response of a marginally stable, ideal peeling mode has been proposed as a candidate to explain the experimental observation [3]. Fig.3 (right), shows simulated RFA depending on beta and the normalised current density at the plasma edge. The non-monotonic behaviour of RFA seen in experiment is also seen in the MARS-F simulations. As the RWM is deeply stable because of low β_N, the RFA in this case is dominated by the peeling mode response. As in the case discussed earlier, it was shown that the stable peeling mode response is not sensitive to the plasma rotation profile or to the damping model. The peeling mode becomes more stable after the 1st ELM (until the next long ELM-free period, as discussed below), and the RFA decreases. With increasing β_N, the RWM starts to give a dominant contribution to the plasma response. In this case, we observe a sensitive dependence of the RFA amplitude (but not the threshold) on plasma rotation profile and on the damping. So, it was possible to separate contributions from the peeling mode and from the stable RWM, as the contribution of the stable RWM to the RFA was found to be small at low β_N value and increases with β_N. The computed RFA amplitudes largely agree with the experimental measurements shown in Fig.3, with the strongest response at low β_N corresponding to a marginally stable peeling mode. The experimental RFA response, measured at the RFA threshold, was dominantly caused by the stable RWM.

These RFA peaks can potentially be used as an active MHD spectroscopy tool to predict the stability of the Edge Localised Mode. Since the peeling mode response to an applied probing field tends to peak at the marginal stability point, it may be possible to use the RFA measurement in the experiments to predict ELM events caused by the onset of these low-n peeling modes.

2. ROLE OF KINETIC EFFECTS

In order to assess the role of the kinetic effects in damping the RWM, the drift-kinetic HAGIS code [5] has been used to calculate the change in the δW in the presence of trapped and passing ions [4]. The very low mode frequency of the RWM (a few Hz in JET) suggests that particles will interact with the mode at the precession drift frequency, strongly affecting the damping. The effects of the toroidal rotation and pressure gradients upon the kinetic damping of the RWM have also been considered. A weakly damped RWM in the presence of rotation or kinetic damping can amplify the resonant component of applied helical magnetic field [6]. A new model retaining information about the plasma response in comparison with the kinetic damping model describes the resonant field amplification in the presence of a stable RWM [4]. It was compared with the experimental data and has shown good agreement both in the dependence of the RFA amplitude on the applied probing

field frequency at different beta and in the RFA amplitude growth with beta. Potentially, this model can help estimating the damping of the RWM from the RFA data and so predicting what limitation of the plasma performance could be expected if the plasma conditions are changed affecting the damping mechanism during performance optimisation experiments.

3. RFA MEASUREMENTS ON JET AT LOW β_N

Figure 4 shows evolution of RFA in a low beta (β_N~2) pulse with several ELM-free periods. The visible increase in the RFA during ELM-free periods may be connected with the peeling-RWM interplay discussed above. However, there is a pronounced increase in the RFA maximum level. This increase can not be explained by the stable peeling mode response due to changes in the plasma rotation profile or to the damping and the contribution of the RWM at these beta values should be small. A reasonable explanation is in that the plasma is evolving towards the top right corner of the stability diagram in Fig.3 (right), as suggested by the zigzag dotted line. However, this implies a gradual increase in the maximum level of the edge current achieved at ELM-free periods during the pulse. More studies with advanced edge current density profile diagnostics will be needed to confirm this hypothesis. Other possible explanations may be connected with changes in the RWM stability; however there is no evidence of any significant variation of global plasma parameters during the pulse (bottom plot).

Also it is noticeable that the RFA growth is slower than that typically observed at the RFA threshold and is closer to that seen in Fig.3 left, in peaks below the threshold. Fig.5 (left) shows RFA relative growth vs growth time during ELM-free period (which is close to the duration of ELM-free periods) before 1st ELM, and during ELM-free periods at flat-top in two similar pulses 73091 and 73092. Red dash line shows linear fit to the data before the 1st ELM. It is noticeable that during ELM-free periods at flat-top the growth is higher. This is illustrated in Fig.5 (right), where RFA relative growth and RFA growth rate measured as $\Delta RFA/\Delta t^{growth}$ versus time (at RFA_{max}) in Pulse No's: 73091 and 73092 during pulse flat-top are shown. Both the relative amplitude of RFA and the growth rate increase during the pulse, as discussed above.

Another experiment that helps to understand stability prior to the 1st ELM has been performed in high pedestal temperature regime [7]. In these experiments an outer mode (OM) [8] has sometimes been observed before the 1st ELM, Fig.6, and was claimed to delay the appearance of the 1st ELM. The OM affects the pedestal, the edge current density and so the peeling stability. A reduction in the *n = 1* RFA level due to appearance of the *n = 2* outer mode has been found, Fig.6 (top). Here two high temperature pedestal pulses are overlapped, one (Pulse No: 78010, red) with *n = 2* OM bursts at t = 13.8 sec and 14.25 sec, and another (Pulse No: 78009, blue) – without pronounced OM. Reduction in RFA correlated with the OM is clearly seen. As the RFA was measured with *n = 1* and OM has *n = 2*, this reduction in the RFA can not be attributed to the direct pick-up from the OM, but rather to changes in the edge stability. This, like in the case of RFA spike before the onset of slow rotating *n = 1* mode [1], suggests that the RFA is sensitive to stability conditions and does not

just reflect the presence of a mode.

RWM coupling with ELMs has been previously reported in [6]. This suggests that the current density profile modification due to ELMs indeed may affect the RWM stability, and so the ideal no-wall limit.

4. COMPARISON OF *N=1* AND *N=2* PROBING

Figure 7 shows results of *n = 1 and n = 2* probing in similar pulses. The *n = 2* RFA does not grow as much as the *n = 1*, so the *n = 2* limit in these pulses is probably higher than the *n = 1* limit. However, *n = 2* probing before the 1st ELM shows results very similar to those of the *n = 1* probing. Fig.8 shows *n = 2* RFA with pronounced peak at $\beta_N = 1.75$ that corresponds to the 1st ELM. Growth rates for *n = 2* RFA are shown in Fig.5 (left) and they are similar to those of *n=1*. These suggest that stability at 1st ELM is not dominated by *n = 1* and the eigenfunction has multi-mode structure, which is in agreement with the peeling modelling for these JET pulses [3].

CONCLUSIONS

Resonant Field Amplification measurements have been used on JET as an active MHD spectroscopy to probe plasma stability at high and low beta and the results have been compared with theoretical predictions. At high beta, a new method of the no-wall beta limit identification using the logarithmic derivative of the RFA amplitude versus β_N has been proposed and tested. It was found that the beta limit strongly depends on the current density and q profiles, and in particular on the q(0) value for monotonic q-profiles or q_{min} for reversed shear profiles and on details of the current density profile at the plasma edge. This explains experimentally observed significant variation of the RFA threshold and associated ideal stability limit with q(0) or q_{min} and increase in RFA during ELM-free periods which is probably connected with the current density profile (and the peeling stability) changes at the plasma edge. The reduction in the RFA observed in the presence of the outer mode confirms this suggestion.

A new model retaining information about the plasma response in comparison with the kinetic damping model describes the RFA in the presence of a stable RWM. The RFA has been found to be a potentially good indicator of the overall stability, predicting the appearance of a limiting *n = 1* mode and the first ELM even below the ideal no-wall limit, or showing the no-wall ideal beta limit at higher beta which may be useful for predictions of the plasma performance when variations in the damping and stabilising mechanisms can determine operating boundaries in advanced regimes. The first measurements of the plasma response to the *n = 2* probing show good prospects for comparison of the *n = 1* and *n = 2* stability limits.

ACKNOWLEDGEMENTS

This work was carried out within the framework of the European Fusion Development Agreement Work, and partly funded by the UK EPSRC under grant EP/G003955 and the EC under the contract

of Association between EURATOM and CCFE. The views and opinions expressed herein do not necessarily reflect those of the European Commission. This work was carried out within the framework of the European Fusion Development Agreement.

REFERENCES

[1]. M.P. Gryaznevich et al, *Experimental Studies of Stability and Beta Limit in JET,* Plasma Physics and Controlled Fusion **50** (2008) 124030

[2]. Yueqiang Liu, et al, *An Improved Method to Evaluate the Ideal No-Wall Beta Limit from Resonant Field Amplification Measurements in JET*. Plasma Physics and Controlled Fusion **51** (2009) 115005

[3]. Yueqiang Liu, et al, *Modelling Resonant Field Amplification Due to Low-n Peeling Modes in JET*, Plasma Physics and Controlled Fusion **52** (2010) 045011

[4]. I.T. Chapman, et al, *Stability of the Resistive Wall Mode in JET*, Plasma Physics and Controlled Fusion **51** (2009) 055015

[5]. S.D. Pinches et al 1998 Computer Physics Communications **111** 133 (Release Version 8.09)

[6]. D.F. Howell, et al, Proceedings of the 36th EPS Conference on Plasma Physics, Sofia, Bulgaria. (29th June 2009 - 3rd July 2009), EFDA–JET–CP(09)06/05

[7]. E.R. Solano et al, *Observation of Confined Current Ribbon in JET Plasmas,* Physical Review. Letters **104** (2010) 185003

[8]. G.T.A Huysmans, *et al*., Nuclear Fusion **38**, 179 (1998)

[9]. P. Buratti, this Conference, EXS/P5-02

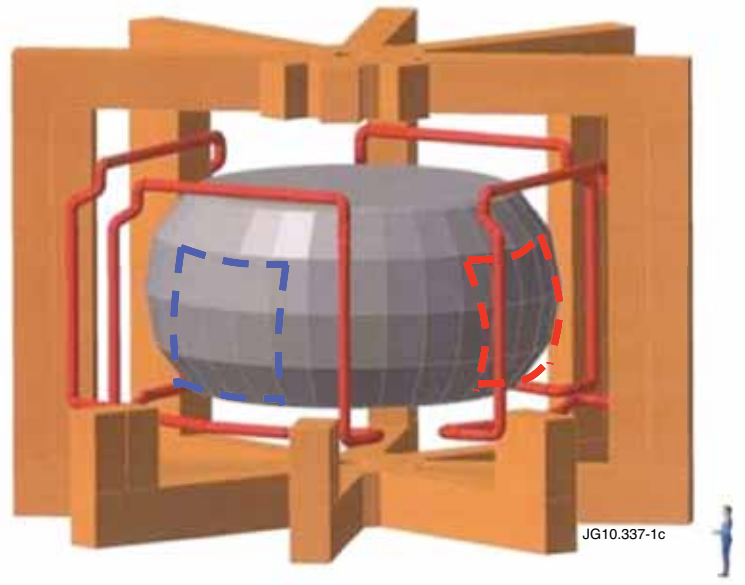

Figure 1: Position of the external Error Field Correction Coils (solid red) and measuring loops (dashed red and blue, only 2 of 4 saddle loops are shown) on JET.

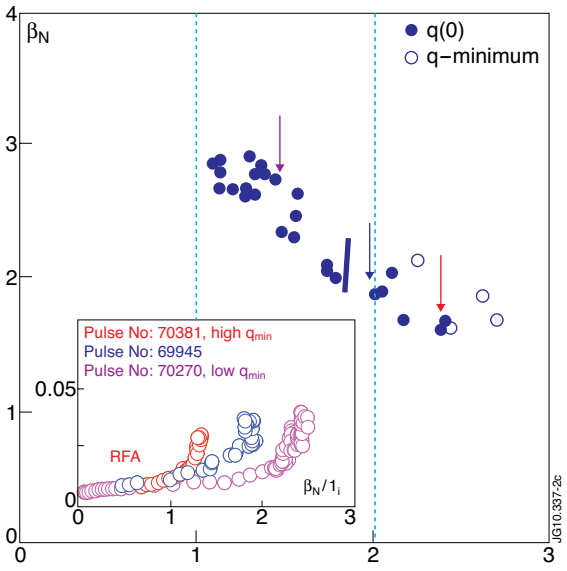

Figure 2: Decrease in RFA threshold measured in the high-β_N low or slightly reversed shear pulses with q_{min} determined using EFIT constrained by MSE, polarimetry, pressure, low-n MHD and Alfven Cascades. Insert: Sudden increase in the RFA, indicating the no-wall limit, does not correlate (at different q_{min}) with integral parameters (e.g. $4l_i$)

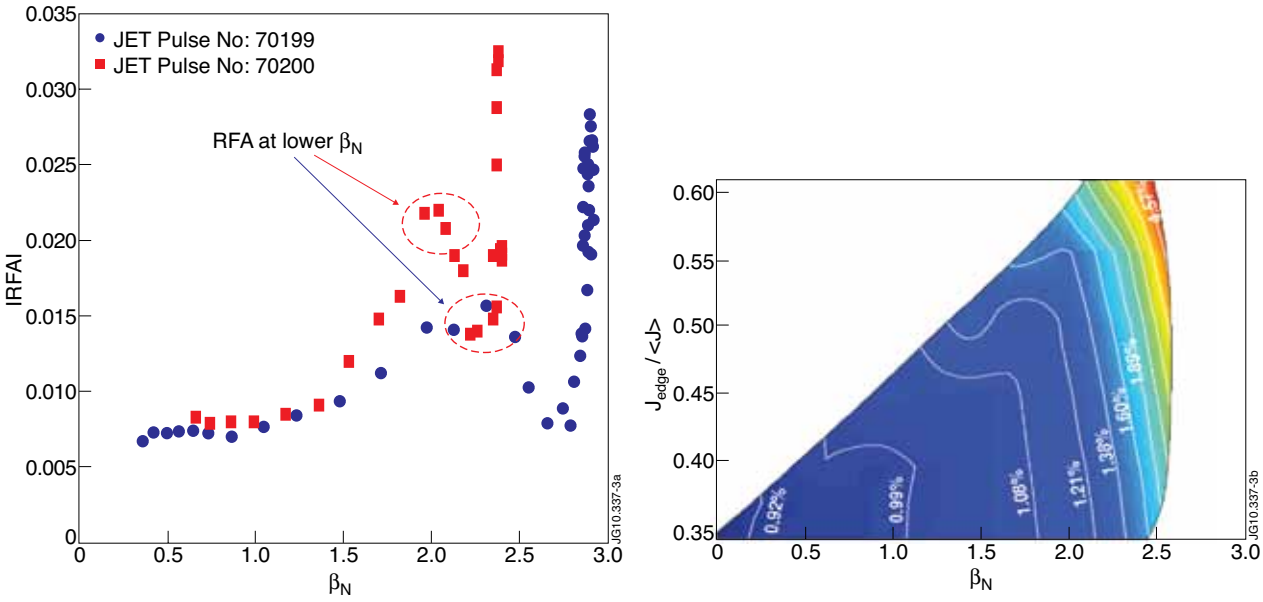

Figure 3: Non-monotonic n=1RFA response observed at low β_N well below the RFA threshold, prior to the 1st ELM, left, and the simulated RFA response (white contours, in %), MARS-F, right. Red zigzag line shows cartoon of a possible edge current evolution, as discussed in Section 3.

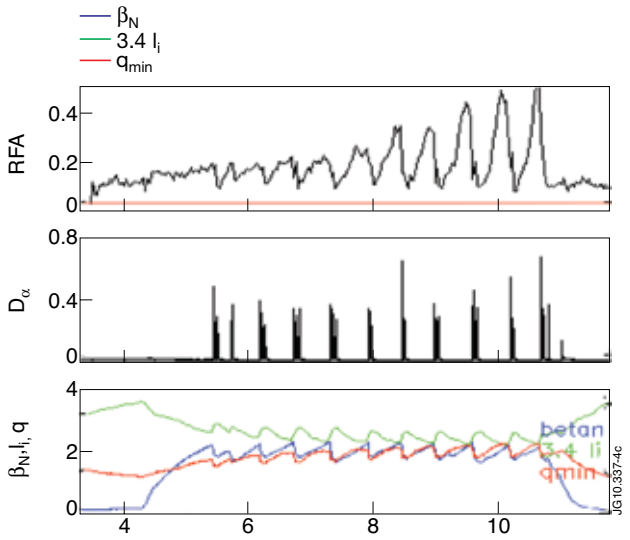

Figure 4: RFA (top) increases during ELM-free period (middle), at constant low β_N (bottom plot), Pulse No:73092. (Plasma pulse starts at t = 40s in this and the next figures).

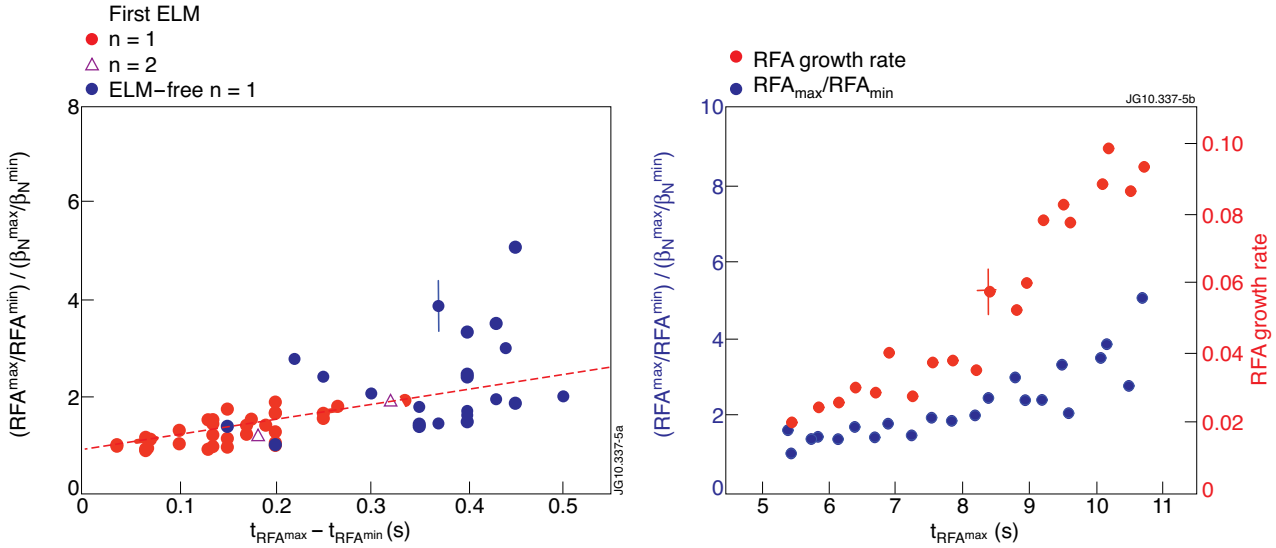

Figure 5: Left: RFA growth versus growth time during ELM-free period before 1st ELM, • n=1, • n=2 and during ELM-free periods at flat-top in Pulse No's: 73091, 73092, • n=1. Red line shows linear fit to the data before 1st ELM. Right: RFA growth and RFA growth rate vs time (at RFA_{max}) in Pulse No: 73091 during pulse flat-top.

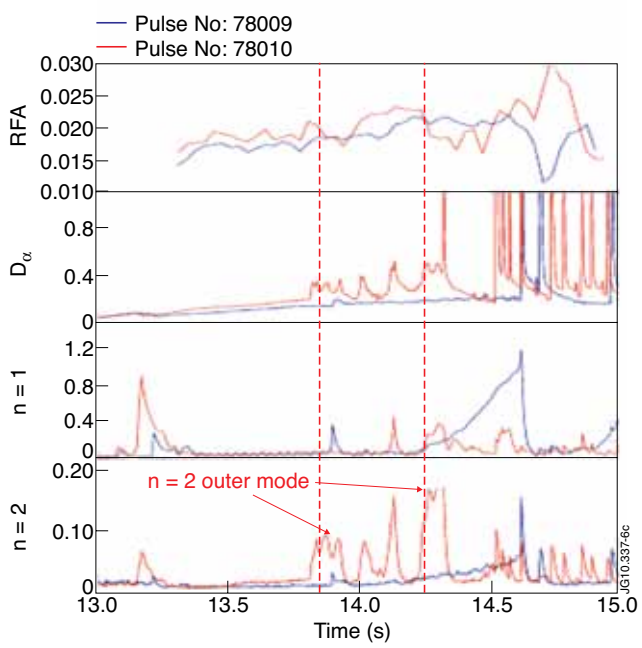

Figure 6: Reduction in RFA observed during the outer mode. From top to bottom: RFA, D_α, n = 1 and n = 2 mode amplitude. Blue – Pulse No:78009, no outer mode, red – Pulse No:78010, with outer mode.

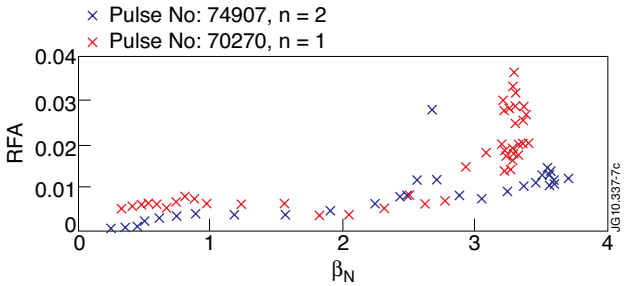

Figure 7: n = 1 and n = 2 probing in similar pulses.

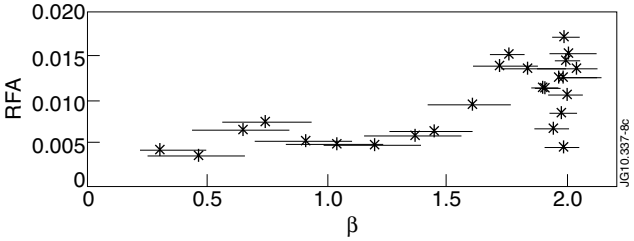

Figure 8: Non-monotonic n=2 RFA response observed prior to the 1st ELM at low β_N below the RFA threshold, Pulse No:75862.